JOURNAL OF COMPUTATIONAL PHYSICS **128,** 32–42 (1996)
ARTICLE NO. 0194

Implicit Lower-Upper/Approximate-Factorization Schemes for Incompressible Flows

W. ROGER BRILEY, SHYAM S. NEERARAMBAM AND DAVID L. WHITFIELD

National Science Foundation Engineering Research Center for Computational Field Simulation, Mississippi State University, Mississippi State, Mississippi 39762

Received May 30, 1995; revised March 13, 1996

A lower-upper/approximate-factorization (LU/AF) scheme is developed for the incompressible Euler or Navier–Stokes equations. The LU/AF scheme contains an iteration parameter that can be adjusted to improve iterative convergence rate. The LU/AF scheme is to be used in conjunction with linearized implicit approximations and artificial compressibility to compute steady solutions, and within sub-iterations to compute unsteady solutions. Formulations based on time linearization with and without sub-iteration and on Newton linearization are developed using spatial difference operators. The spatial approximation used includes upwind differencing based on Roe's approximate Riemann solver and van Leer's MUSCL scheme, with numerically computed implicit flux linearizations. Simple one-dimensional diffusion and advection/diffusion problems are first studied analytically to provide insight for development of the Navier–Stokes algorithm. The optimal values of both time step and LU/AF parameter are determined for a test problem consisting of two-dimensional flow past a NACA 0012 airfoil, with a highly stretched grid. The optimal parameter provides a consistent improvement in convergence rate for four test cases having different grids and Reynolds numbers and, also, for an inviscid case. The scheme can be easily extended to three dimensions and adapted for compressible flows.

1. INTRODUCTION

The solution of both steady and unsteady incompressible viscous flows has benefited from the artificial compressibility formulation of Chorin [1]. Examples of methods using artificial compressibility are given in [2–6]. With artificial compressibility, the use of linearized implicit methods solved using ADI or relaxation schemes is very similar to established methods for compressible flows. Steady solutions can be obtained using iteration in time or relaxation, and unsteady solutions can employ sub-iteration procedures [2, 3, 5, 6] based on artificial compressibility. The linearized implicit equations which arise are often addressed using variants of approximate factorization or relaxation. Jameson and Turkel [7] suggested implicit LU schemes expressed as approximate factorizations which have two factors in three dimensions instead of the three factors associated with ADI schemes. The symmetric Gauss–Seidel relaxation scheme can also be expressed as an LU approximate factorization (see, for example, Jameson [8]). LU schemes are used in the incompressible methods of [3, 5, 9–13]. The treatment of diffusion terms in LU schemes is considered in [14].

In the present paper, a modified LU approximate factorization is developed for use in conjunction with linearized implicit approximations and artificial compressibility to compute steady or unsteady solutions of the incompressible Navier–Stokes equations. The purpose of the modified LU/AF scheme is the introduction of an iteration parameter α which can be adjusted to improve the iterative convergence rate. For one choice of the parameter ($\alpha = 1$), this scheme is equivalent to symmetric Gauss–Seidel relaxation; for another choice ($\alpha = 0$), the factorization is an LU analog of that used in ADI schemes. Optimal convergence behavior is found to occur at an intermediate value of the parameter. The scheme can be used with or without sub-iteration at each time step. Formulations based on both time-linearization and Newton linearization are given.

The spatial approximation and numerically computed flux Jacobians used here are the same as those given by Whitfield and Taylor in [11]. A finite volume approximation in transformed coordinates is used, with upwind differencing based on Roe's [15] approximate Riemann solver (adapted for the artificial compressibility equations) and van Leer's [16] MUSCL scheme, following Anderson, Thomas, and van Leer [17]. Flux Jacobians are computed numerically as suggested by Whitfield and Taylor in [18].

The present paper is organized as follows: Section 2 contains analytical results for simple one-dimensional diffusion and advection/diffusion problems. Section 3 contains the two-dimensional governing equations in transformed coordinates. In Section 4, iterative formulations which distinguish time linearization and Newton linearization are developed, along with a general statement of the approximate factorization. The numerical flux and Jacobian approximations are given in Section 5, and definition of the LU/AF scheme is completed in Section 6. Computed results for a two-dimensional airfoil problem are given in Section 7.

0021-9991/96 $18.00

2. MODEL PROBLEM RESULTS

2.1. *Implicit Algorithm for a One-Dimensional Diffusion Equation*

Consider the one-dimensional diffusion equation:

$$\frac{\partial q}{\partial t} = \nu \frac{\partial^2 q}{\partial x^2}, \tag{2.1}$$

where ν is constant. Assume a discretization with constant time step Δt and grid spacing Δx, such that $q_i^n = q(n\Delta t, i\Delta x)$. The following implicit approximation is obtained using Euler implicit time differencing and central space differences,

$$(C^{-1} - \delta_i^2)\Delta q^n = \delta_i^2 q^n, \tag{2.2}$$

where $C \equiv \nu\Delta t/(\Delta x)^2$, $\Delta q^n \equiv q^{n+1} - q^n$, and δ is the central difference operator.

2.2. *LU Approximate Factorization Scheme*

Although the tridiagonal system associated with (2.2) is easily solved, the present objective is to gain insight into an LU/AF scheme to motivate and guide its application to the multidimensional Navier–Stokes equations, where fully implicit solutions are not so economically solved. Accordingly, an approximate factorization of (2.2) is considered which can be written symbolically as

$$[D + \mathscr{L}_1(\cdot)]D^{-1}[D + \mathscr{L}_2(\cdot)]\Delta q^n = \delta_i^2 q^n \equiv r(q^n). \tag{2.3}$$

Here, D is a scalar quantity, r is the spatial residual operator, and $\mathscr{L}_1$ and $\mathscr{L}_2$ are difference operators. The present LU/AF scheme is defined by (2.3) and

$$D(\cdot) = (C^{-1} + 2\alpha)(\cdot)_i \tag{2.4a}$$

$$\mathscr{L}_1(\cdot) = -(\cdot)_{i-1} + (1 - \alpha)(\cdot)_i \tag{2.4b}$$

$$\mathscr{L}_2(\cdot) = -(\cdot)_{i+1} + (1 - \alpha)(\cdot)_i. \tag{2.4c}$$

A free parameter α whose purpose is to accelerate convergence to a steady solution has been included in this scheme. For $\alpha = 0$, the scheme is analogous to an ADI type of approximate factorization with *directions* given by backward and forward differences such that $\mathscr{L}_1 = \nabla_i$, $\mathscr{L}_2 = -\Delta_i$. For $\alpha = 1$, the scheme can be shown to be equivalent to symmetric Gauss–Seidel (SGS) relaxation as $C \to \infty$. The approximate factorization can be solved for Δq_i^n in two steps which are associated with lower and upper triangular matrices (hence, the LU/AF designation). These steps can be written more directly as

$$(C^{-1} + 1 + \alpha)\Delta q_i^* - \Delta q_{i-1}^* = q_{i-1}^n - 2q_i^n + q_{i+1}^n \tag{2.5a}$$

$$(C^{-1} + 1 + \alpha)\Delta q_i^n - \Delta q_{i+1}^n = (C^{-1} + 2\alpha)\Delta q_i^*. \tag{2.5b}$$

2.3. *Analysis of Asymptotic Iterative Convergence Rate*

The convergence of the above scheme is analyzed to determine optimal values of the parameter α. If $\bar{q}$ is the steady solution to (2.3), then the error ε^n at each step is given by $\varepsilon_i^n = q_i^n - \bar{q}_i$. Since the governing equation is linear, this error ε_i^n satisfies the same difference equation as the solution q_i^n. If the boundary conditions are assumed to be *homogeneous* Dirichlet conditions, then the error can be expressed as a Fourier series for an odd function on a discrete half interval in space, as

$$\varepsilon_i = \sum_{k=1}^{N-1} b_k \sin(\omega_k x_i); \quad i = 0, 1, 2, ..., N, \tag{2.6}$$

where $\omega_k = k\pi$, $x_i = i\Delta x$, and $\Delta x = 1/N$. Assuming the initial solution satisfies the boundary conditions, then each Fourier error component will also satisfy the homogeneous Dirichlet conditions, and the results from a Fourier or von Neumann stability analysis can also be used for analysis of iterative convergence. Substituting a typical Fourier component of the form

$$\varepsilon_i^n = z_k^n \sin(\omega_k x_i) \tag{2.7}$$

into (2.3) leads to the expression for the amplification factor z_k for each error components,

$$z_k = \frac{1 + 2\alpha C + C^2[\alpha^2 + (1 - \alpha)\sigma_k]}{(1 + \sigma_k C)(1 + 2\alpha C) + C^2[\alpha^2 + (1 - \alpha)\sigma_k]}, \tag{2.8}$$

where $\sigma_k = 4 \sin^2(k\pi/2N)$. Analysis of (2.8) gives the following results:

a. The lowest frequency error ($k = 1$) has the largest amplification factor and, hence, governs the convergence rate. Thus, $\sigma_1 = 4 \sin^2(\pi/2N) \approx (\pi/N)^2$.

b. For $\alpha = 0$ (ADI type), the scheme has an optimal time step given by $C_{\text{opt}} = 1/\sqrt{\sigma_1}$, and spectral radius of $z_{\text{opt}} = (1 + 2\sqrt{\sigma_1})^{-1}$, with slower convergence at both smaller and larger C.

c. For $\alpha = 1$ (SGS type), the convergence is very good for a range of C extending to infinity, with $C_{\text{opt}} \to \infty$, and $z_{\text{opt}} = (1 + 2\sigma_1)^{-1}$.

d. For other values of α, the fastest convergence occurs as $C \to \infty$, and the optimal value of α is found to be $\alpha_{\text{opt}} = \sqrt{\sigma_1}$, and $z_{\text{opt}} = (2 - \sqrt{\sigma_1})/(2 + \sqrt{\sigma_1})$.

The asymptotic convergence rate is illustrated by the number of iterations K to reduce the error by a given (arbitrary)

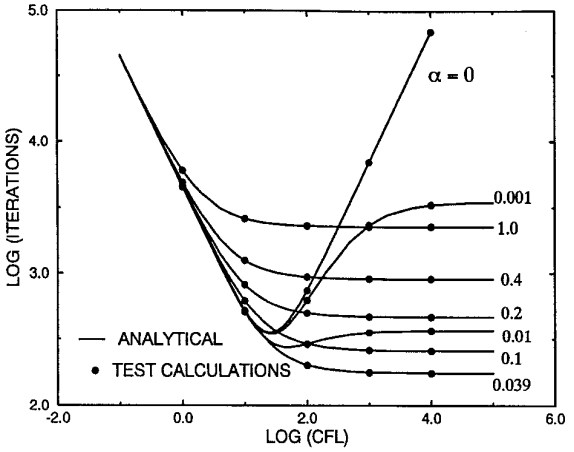

FIG. 1. LU/AF scheme for one-dimensional diffusion equation: Iterations for convergence to 10^{-3} for uniform grid with 80 intervals.

factor γ, which is given by $K = \log(\gamma)/\log(z_{k=1})[\varrho(M)]$. This convergence rate for $N = 80$ and $\gamma = 10^{-3}$ is shown in Fig. 1 for different values of C and α. The analytical results are also compared with asymptotic convergence rates obtained from test calculations using the actual algorithm. In these calculations, the spectral radius of the error reduction matrix was deduced by noting that repeated application of the algorithm is equivalent to the power method for determining the spectral radius of a matrix (see, for example, Jennings [19]). Note in Fig. 1 that the optimal α is very effective in improving the convergence rate for large C.

2.4. *LU/AF Scheme for a One-Dimensional Advection/Diffusion Equation*

The preceding analytical solution is exact and provides relevant insight into the convergence rate as influenced by α and the viscous Courant number C. Further insight into the behavior of this algorithm for high Reynolds number viscous flow is obtained from the following (nondimensional) linear advection/diffusion equation,

$$\frac{\partial q}{\partial t} = -u(x)\frac{\partial q}{\partial x} + \frac{1}{\mathrm{Re}}\frac{\partial^2 q}{\partial x^2}, \tag{2.9}$$

where $u(x)$ is a prescribed velocity distribution ($0 \le u, x \le 1$). Here, the velocity $u(x)$ is specified from the classical Heimenz similarity solution for flow toward a stagnation point (see [20]) and is the distribution along the stagnation streamline of the velocity component normal to the wall. A shear-layer of thickness $\delta = 10^{-2}$ is obtained by taking the Reynolds number as 57,360. A nonuniform grid of 80 mesh increments is used, having a minimum spacing of 7.96×10^{-5} at the wall and maximum spacing of 4.91×10^{-2} at the freestream boundary (giving a mesh ratio of $\Delta x_{\max}/\Delta x_{\min} = 6.17 \times 10^2$). This model problem corresponds to a high Reynolds number flow with well-resolved thin-shear-layer and freestream regions (27 of 81 points are in the shear layer) and has relevance to the region near a stagnation point for many viscous flow problems.

An LU/AF scheme similar to (2.3)–(2.4) is constructed for (2.9) using a finite-volume discretization and a first-order (two-point) upwind approximation for the advection term. This scheme can be written as

$$[D + \mathscr{L}_1(\cdot)]D^{-1}[D + \mathscr{L}_2(\cdot)]\Delta q^n = r(q^n), \tag{2.10}$$

where $r(q^n)$ approximates the RHS of (2.9) and

$$D(\cdot) = \Delta t^{-1} + \alpha(a_{i-1/2} + b_{i+1/2}) \tag{2.11a}$$

$$\mathscr{L}_1(\cdot) = -a_{i-1/2}(\cdot)_{i-1} + (1-\alpha)a_{i-1/2}(\cdot)_i \tag{2.11b}$$

$$\mathscr{L}_2(\cdot) = -b_{i+1/2}(\cdot)_{i+1} + (1-\alpha)b_{i+1/2}(\cdot)_i \tag{2.11c}$$

$$a_{i-1/2} = \frac{1}{\Delta x_{i,\mathrm{avg}}}\left(u_{i-1/2} + \frac{1}{\mathrm{Re}\,\Delta x_{i-1/2}}\right),$$

$$b_{i1/2} = \frac{1}{\Delta x_{i,\mathrm{avg}}}\left(\frac{1}{\mathrm{Re}\,\Delta x_{i+1/2}}\right) \tag{2.11d), (2.11e)}$$

The matrix method is used to determine the iterative rate of convergence of the scheme (2.11) with Dirichlet boundary conditions. The implicit scheme and boundary conditions for all grid points can be expressed in matrix form as $\mathbf{q}^{n+1} = \mathbf{M}\mathbf{q}^n + \mathbf{b}$, where $\mathbf{M}$ is the iteration matrix. The spectral radius $\varrho(M)$ determines the asymptotic rate of convergence and was computed using RG, a subroutine available from CRAY's EISPACK library. The number

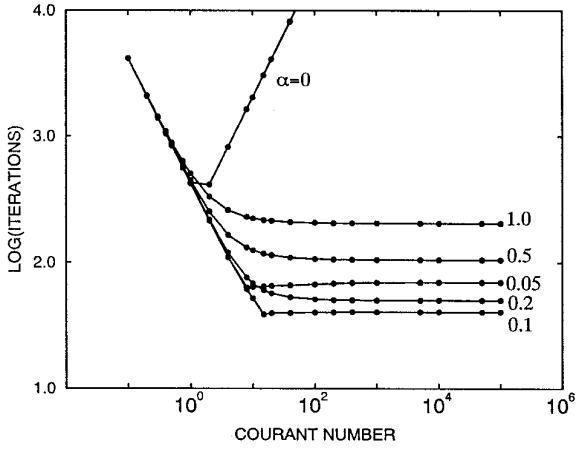

FIG. 2. LU/AF scheme for one-dimensional advection/diffusion equation: Iterations for convergence to 10^{-3} for uniform grid with 80 intervals.

of iterations K to reduce the error by a given factor γ is given by $K = \log(\gamma)/\log[\varrho(M)]$. Results for different α are shown for $\gamma = 10^{-3}$ in Fig. 2, where the Courant number C is given by $C = u_{\text{avg}}\,\Delta t/\Delta x_{\text{avg}}$. A comparison of Figs. 1 and 2 indicates that the convergence behavior for the advection/diffusion equation (2.9) with nonuniform grid and high Reynolds number is qualitatively the same as for the diffusion equation (2.1). If the diffusion term in (2.9) were omitted from this model problem, then $b_{i+1/2}$ would be zero, and Eq. (2.11c) would reduce to zero. There would be no factorization error and, consequently, the solution would converge in one iteration as $\Delta t \to \infty$. Note that these latter observations would not apply if the velocity distribution were to include a change of direction and do not apply to the Euler equations, where eigenvalues of the flux Jacobians have different signs. Thus, diffusion is largely responsible for the dependence of convergence on α in Fig. 2. Both model problems have relevance to the Navier–Stokes equations, where a similar dependence on α will be demonstrated.

3. TWO-DIMENSIONAL INCOMPRESSIBLE NAVIER–STOKES EQUATIONS

An artificial compressibility formulation [2, 5, 6, 10, 11] for the two-dimensional incompressible Navier–Stokes equations, written following a transformation from Cartesian coordinates (x, y, z, t) to dynamic curvilinear coordinates $[\xi(x, y, t), \eta(x, y, t), \tau = t]$ can be written in nondimensional form as

$$\frac{\partial \mathbf{q}}{\partial \tau} + \frac{\partial \mathbf{f}}{\partial \xi} + \frac{\partial \mathbf{g}}{\partial \eta} = 0. \tag{3.1}$$

Here, $\mathbf{q}$ is the vector of dependent variables, $\mathbf{f} = \mathbf{f}_{\text{I}} + \mathbf{f}_{\text{V}}$ and $\mathbf{g} = \mathbf{g}_{\text{I}} + \mathbf{g}_{\text{V}}$ are flux vectors which include both inviscid and viscous flux contributions, and

$$\mathbf{q} = J\begin{pmatrix} p \\ u \\ v \end{pmatrix}, \quad \mathbf{f}_{\text{I}} = J\begin{pmatrix} \beta(U - \xi_t) \\ uU + \xi_x p \\ vU + \xi_y p \end{pmatrix}, \quad \mathbf{g}_{\text{I}} = J\begin{pmatrix} \beta(V - \eta_t) \\ uV + \eta_x p \\ vV + \eta_y p \end{pmatrix} \tag{3.2}$$

$$U = \xi_t + \xi_x u + \xi_y v, \quad V = \eta_t + \eta_x u + \eta_y v \tag{3.3}$$

$$\mathbf{f}_{\text{V}} = J\begin{pmatrix} 0 \\ \xi_x \tau_{xx} + \xi_y \tau_{xy} \\ \xi_x \tau_{yx} + \xi_y \tau_{yy} \end{pmatrix}, \quad \mathbf{g}_{\text{V}} = J\begin{pmatrix} 0 \\ \eta_x \tau_{xx} + \eta_y \tau_{xy} \\ \eta_x \tau_{yx} + \eta_y \tau_{yy} \end{pmatrix} \tag{3.4}$$

$$\begin{aligned} \tau_{xx} &= 2\mu \text{Re}^{-1}[\xi_x u_\xi + \eta_x u_\eta] \\ \tau_{yy} &= 2\mu \text{Re}^{-1}[\xi_y v_\xi + \eta_y v_\eta] \\ \tau_{xy} &= \tau_{yx} = \mu \text{Re}^{-1}[(\xi_y u_\eta + \eta_y u_\eta) + (\xi_x v_\xi + \eta_x v_\eta)]. \end{aligned} \tag{3.5}$$

Here, β is an artificial compressibility parameter, Re is a reference Reynolds number, $J = x_\xi y_\eta - y_\xi x_\eta$ is the Jacobian of the inverse coordinate transformation, and the metric quantities are given by

$$\begin{aligned} J\xi_x &= y_\eta, \quad J\xi_y = -x_\eta, \quad \xi_t = -x_\tau \xi_x - y_\tau \xi_y \\ J\eta_x &= -y_\xi, \quad J\eta_y = x_\xi, \quad \eta_t = -x_\tau \eta_x - y_\tau \eta_y. \end{aligned} \tag{3.6}$$

The artificial time derivative has been added, following the coordinate transformation to ensure that a divergence-free solution is obtained for a dynamic grid.

4. NUMERICAL FORMULATIONS

4.1. *Finite-Volume Approximation*

The following finite-volume approximation of (3.1) is used [2, 5, 6, 10]:

$$\frac{\partial \mathbf{q}}{\partial \tau} = -(\delta_i \mathbf{f} + \delta_j \mathbf{g}) = -\mathbf{R}(\mathbf{q}). \tag{4.1}$$

Here, δ is the central difference operator such that

$$\begin{aligned} \delta_i(\cdot) &\equiv (\cdot)_{i+1/2} - (\cdot)_{i-1/2} \\ \delta_j(\cdot) &\equiv (\cdot)_{j+1/2} - (\cdot)_{j-1/2}. \end{aligned} \tag{4.2}$$

$\mathbf{R}$ denotes a residual operator, and $\Delta\xi$ and $\Delta\eta$ are taken as unity. Here and throughout this paper, nonincremented subscripts are often omitted for simplicity. For example, $\mathbf{q}_i$ is equivalent to $\mathbf{q}_{i,j}$, and $\mathbf{q}_{j+1}$ is equivalent to $\mathbf{q}_{i,j+1}$.

4.2. *Time-Linearized Implicit Formulation*

A first-order backward Euler implicit scheme for (4.1) is given by

$$\Delta \mathbf{q}^n \equiv \mathbf{q}^{n+1} - \mathbf{q}^n = -\Delta\tau \mathbf{R}(\mathbf{q}^{n+1}). \tag{4.3}$$

A time linearization [21] about $\mathbf{q}^n$,

$$\mathbf{R}(\mathbf{q}^{n+1}) = \mathbf{R}(\mathbf{q}^n) + \mathscr{L}^n(\Delta \mathbf{q}^n) + O(\Delta \mathbf{q}^n)^2, \tag{4.4}$$

leads to the following time-linearized implicit formulation:

$$[I/\Delta\tau + \mathscr{L}^n(\cdot)]\Delta \mathbf{q}^n = -\mathbf{R}(\mathbf{q}^n). \tag{4.5}$$

Here, $\mathscr{L}^n$ is a linear operator representing $\partial \mathbf{R}/\partial \mathbf{q}$, to be specified in detail in Section 6. A steady solution of (4.1) is obtained as $\Delta \mathbf{q}^n \to 0$. Although the present paper considers only two-point first-order accurate time differencing, a straightforward modification using three-point backward time differences as in [2, 6, 10] would give second-order time accuracy.

4.3. *Generalized Approximate Factorization Algorithm*

Direct solution of (4.5) is uneconomical for large problems, and so an approximate factorization of the left-hand side is introduced. The approximate factorization scheme can be written in the general form

$$[D + \mathscr{L}_1^n(\cdot)]D^{-1}[D + \mathscr{L}_2^n(\cdot)]\Delta\mathbf{q}^n = -\mathbf{R}(\mathbf{q}^n). \quad (4.6)$$

Here, D is a matrix, and $\mathscr{L}_1$ and $\mathscr{L}_2$ are difference operators which should satisfy

$$D(\cdot) + \mathscr{L}_1^n(\cdot) + \mathscr{L}_2^n(\cdot) = (I/\Delta\tau)(\cdot) + \mathscr{L}^n(\cdot). \quad (4.7)$$

Specific definitions of D, $\mathscr{L}_1$, and $\mathscr{L}_2$ appropriate for a one-parameter LU/AF scheme of the type introduced in Section 1 will be given in Section 6, once flux approximations and flux Jacobians have been defined. With D, $\mathscr{L}_1$, and $\mathscr{L}_2$ specified, Eq. (4.6) can be solved in two steps:

$$[D + \mathscr{L}_1^n(\cdot)]\Delta\mathbf{q}^* = -\mathbf{R}(\mathbf{q}^n) \quad (4.8a)$$

$$[D + \mathscr{L}_2^n(\cdot)]\Delta\mathbf{q}^n = D\Delta\mathbf{q}^*. \quad (4.8b)$$

4.4. *Iterative Time-Linearized Implicit Formulation*

Letting m denote a sub-iteration index ($m = 0, 1, \ldots$) and using the shorthand notation,

$$\psi^{m+1} \equiv (\Delta\mathbf{q}^n)^{m+1} = \mathbf{q}^{n+1,m+1} - \mathbf{q}^n, \quad (4.9)$$

an iterative nonlinear implicit formulation of Eq. (4.3) can be written as

$$\psi^{m+1} = -\Delta\tau\mathbf{R}(\mathbf{q}^{n+1,m+1}). \quad (4.10)$$

A time linearization about $\mathbf{q}^n$,

$$\mathbf{R}(\mathbf{q}^{n+1,m+1}) = \mathbf{R}(\mathbf{q}^n) + \mathscr{L}^n(\psi^{m+1}) + O(\psi^{m+1})^2 \quad (4.11)$$

leads to the iterative time-linearized implicit formulation analogous to (4.5),

$$[I/\Delta\tau + \mathscr{L}^n(\cdot)]\psi^{m+1} = -\mathbf{R}(\mathbf{q}^n). \quad (4.12)$$

This can be rewritten in incremental form as

$$[I/\Delta\tau + \mathscr{L}^n(\cdot)]\Delta\psi^m = -\mathbf{R}(\mathbf{q}^n) - [I/\Delta\tau + \mathscr{L}^n(\cdot)]\psi^m, \quad (4.13)$$

where $\Delta\psi^m \equiv \psi^{m+1} - \psi^m$. The LU/AF scheme in (4.6) can also be applied to Eq. (4.13). Note that an unsteady time-linearized solution satisfying (4.5) is obtained as the sub-iteration converges ($\Delta\psi^m \to 0$). The artificial compressibility approximation in the time derivatives can be removed from this unsteady solution if I is replaced by $I_a \equiv$ diag (0, 1, 1) on the right-hand side of (4.13), as suggested, for example, in [2, 6, 10]. Also if the initial value $\psi^{m=0}$ is taken as zero, then the last bracketed term in (4.13) disappears and, thus, a single iteration of (4.13) is equivalent to Eq. (4.5). Note that the sub-iteration serves to remove the factorization error, but not the $O(\Delta\tau)^2$ linearization error.

The LU/AF scheme applied to (4.13) gives

$$[D + \mathscr{L}_1^n(\cdot)]\Delta\psi^* = \text{RHS of (4.13)} \quad (4.14a)$$

$$[D + \mathscr{L}_2^n(\cdot)]\Delta\psi^m = D\Delta\psi^*. \quad (4.14b)$$

The above scheme can be rewritten to solve for ψ instead of $\Delta\psi$. For example, replace (4.14b) by the sum of (4.14a) and (4.14b), and then replace $\Delta\psi$ by the appropriate difference in ψ. Exploiting cancellation which occurs as a result of (4.7), the following two steps equivalent to (4.14a), (4.14b) are obtained:

$$[D + \mathscr{L}_1^n(\cdot)]\psi^* \quad + \mathscr{L}_2^n(\psi^m) = -\mathbf{R}(\mathbf{q}^n) \quad (4.15a)$$

$$[D + \mathscr{L}_2^n(\cdot)]\psi^{m+1} + \mathscr{L}_1^n(\psi^*) = -\mathbf{R}(\mathbf{q}^n). \quad (4.15b)$$

Solution of (4.15a), (4.15b) is more efficient than (4.14a), (4.14b) (assumming the residual is saved) because of the complexity of RHS(4.13). Also, note that if $\mathscr{L}_1$ and $\mathscr{L}_2$ lead to strictly lower and upper matrices, respectively, then (4.15) is a symmetric Gauss–Seidel iteration for solving (4.12) and, hence, (4.5).

4.5. *Iterative Newton-Linearized Implicit Formulation*

Letting s denote a Newton-iteration index, the iterative nonlinear implicit formulation (4.10) can be written as

$$\psi^{s+1} = -\Delta\tau\mathbf{R}(\mathbf{q}^{n+1,s+1}). \quad (4.16)$$

A Newton linearization about $\mathbf{q}^{n+1,s}$,

$$\mathbf{R}(\mathbf{q}^{n+1,s+1}) = \mathbf{R}(\mathbf{q}^{n+1,s}) + \mathscr{L}^{n+1,s}(\Delta\psi^s) + O(\Delta\psi^s)^2, \quad (4.17)$$

leads to Newton's method for the unsteady solution of the *nonlinear* scheme (4.3) (see, for example, [18]):

$$[I/\Delta\tau + \mathscr{L}^{n+1,s}(\cdot)]\Delta\psi^s = -[I/\Delta\tau\,\psi^s + \mathbf{R}(\mathbf{q}^{n+1,s})]. \quad (4.18)$$

Again, the artificial compressibility approximation in the time derivatives can be removed from this unsteady solution if I is replaced by I_a on the right-hand side of (4.18). Also, as $\Delta\tau \to \infty$ this formulation becomes Newton's method for computing a steady solution $\mathbf{R}(\mathbf{q}) = 0$.

To solve for the Newton iterates, a sub-iteration with

index m is introduced, and the result is written in incremental form as

$$\begin{aligned}[I/\Delta\tau + \mathscr{L}^{n+1,s}(\cdot)]\Delta_m(\Delta\psi^s) \\ = -[I/\Delta\tau\,\psi^s + \mathbf{R}(\mathbf{q}^{n+1,s})] \\ - [I/\Delta\tau + \mathscr{L}^{n+1,s}(\cdot)](\Delta\psi^s)^m.\end{aligned} \tag{4.19}$$

As $\Delta_m(\Delta\psi^s) \to 0$ this scheme converges to the Newton increment $\Delta\psi^s$ in (4.18).

The LU/AF scheme in (4.6) can be applied to the subiterative Newton formulation (4.19) and, when implemented as in (4.15), gives

$$\begin{aligned}[D + \mathscr{L}_1^{n+1,s}(\cdot)](\Delta\psi^s)^* \\ + \mathscr{L}_2^{n+1,s}(\Delta\psi^s)^m = \text{RHS of (4.18)}\end{aligned} \tag{4.20a}$$

$$\begin{aligned}[D + \mathscr{L}_2^{n+1,s}(\cdot)](\Delta\psi^s)^{m+1} \\ + \mathscr{L}_1^{n+1,s}(\Delta\psi^s)^* = \text{RHS of (4.18)}\end{aligned} \tag{4.20b}$$

5. NUMERICAL FLUX AND JACOBIAN APPROXIMATIONS

5.1. *Numerical Flux Approximation*

An upwind differencing based on Roe's [15] approximate Riemann solver is used for inviscid fluxes. The approximation is based on van Leer's [16] MUSCL scheme, following [11, 17]. The approximation assumes that waves move normal to the cell faces in each direction. For the ξ direction, Roe's approximation can be written as

$$\mathbf{f}_{I_{i+1/2}} = \mathbf{f}_{I_{i+1/2}}(\mathbf{q}^L_{i+1/2}) + \overline{\mathbf{A}}^-_{i+1/2}(\mathbf{q}_{i+1/2}) \cdot (\mathbf{q}^{\mathrm{R}}_{i+1/2} - \mathbf{q}^{\mathrm{L}}_{i+1/2}) \tag{5.1}$$

Here, $\overline{A}^-$ is a matrix formed from the eigensystem of the inviscid flux Jacobian $\mathbf{A} \equiv \partial\mathbf{f}_{\mathrm{I}}/\partial\mathbf{q}$ as

$$\overline{\mathbf{A}}^{\pm} = \mathbf{S}\Lambda^{\pm}\mathbf{S}^{-1}, \tag{5.2}$$

where $\mathbf{S}$ is a matrix whose columns are the right eigenvectors of $\overline{\mathbf{A}}$, and Λ is a diagonal matrix whose nonzero diagonal elements contain the positive (Λ^+) or negative (Λ^-) eigenvalues of $\overline{A}$. The eigensystem of $\overline{\mathbf{A}}$ is given in [2, 10]. The matrix $\overline{\mathbf{A}}^-$ is evaluated using Roe-averaged variables, which for the incompressible case are defined by

$$\mathbf{q}_{i+1/2} = \tfrac{1}{2}(\mathbf{q}^{\mathrm{R}}_{i+1/2} + \mathbf{q}^{\mathrm{L}}_{i+1/2}). \tag{5.3}$$

The solution to the right ($\mathbf{q}^{\mathrm{R}}$) and left ($\mathbf{q}^{\mathrm{L}}$) of a cell face is evaluated from the van Leer MUSCL formulation [11, 17],

$$\mathbf{q}^{\mathrm{R}}_{i+1/2} = \mathbf{q}_{i+1} - \frac{\phi}{4}[(1-\chi)(\mathbf{q}_{i+2} - \mathbf{q}_{i+1}) + (1+\chi)(\mathbf{q}_{i+1} - \mathbf{q}_i)] \tag{5.4a}$$

$$\mathbf{q}^{L}_{i+1/2} = \mathbf{q}_i + \frac{\phi}{4}[(1-\chi)(\mathbf{q}_i - \mathbf{q}_{i-1}) + (1+\chi)(\mathbf{q}_{i+1} - \mathbf{q}_i)]. \tag{5.4b}$$

The accuracy of these formulas is first-order if $\phi = 0$; second-order if $\phi = 1$, $\chi = -1$; and third-order if $\phi = 1$, $\chi = \frac{1}{3}$.

Definitions analogous to those in (5.1)–(5.4) for the ξ direction follow immediately for the η direction formulas by replacing i by j, $\mathbf{f}_I$ by $\mathbf{g}_I$, $\overline{\mathbf{A}}$ by $\overline{\mathbf{B}}$ (where $\mathbf{B} \equiv \partial\mathbf{g}_I/\partial\mathbf{q}$), and using the eigensystem for $\overline{\mathbf{B}}$ to define

$$\overline{\mathbf{B}}^{\pm} = \mathbf{T}\Lambda^{\pm}\mathbf{T}^{-1}. \tag{5.5}$$

For the viscous fluxes, a centered approximation is used, as described in [10].

5.2. *Numerical Flux Jacobians*

Linearization of the different implicit schemes requires some form of the flux Jacobian matrix, denoted $\mathbf{f}'(\mathbf{q}) \equiv \partial\mathbf{f}/\partial\mathbf{q}$. The analytical determination of the *inviscid* flux Jacobian for Roe's method is not generally tractable and, thus, Whitfield and Taylor [18] suggest computing them numerically, a technique commonly used with Newton's method (Ortega and Reinboldt [22]). If storage is available, the cost of the numerical Jacobians can be mitigated by reuse and infrequent updating (an approximate Newton's method).

The inviscid flux $\mathbf{f}_{I_{i+1/2}}$ depends on $\mathbf{q}_i$ and $\mathbf{q}_{i+1}$ for the first-order approximation (a two-point grid stencil), and the higher order approximations depend on $\mathbf{q}_{i-1}$, $\mathbf{q}_i$, $\mathbf{q}_{i+1}$, and $\mathbf{q}_{i+2}$ (a four-point stencil). The viscous flux $\mathbf{f}_{V_{i+1/2}}$ depends on $\mathbf{q}_i$, $\mathbf{q}_{i+1}$, $\mathbf{q}_{i,j\pm1}$, and $\mathbf{q}_{i+1,j\pm1}$ (a six-point stencil). Although a formal linearization would require a flux Jacobian for the variation of $\mathbf{f}$ with $\mathbf{q}$ at each point in the grid stencil, in practice (cf. [11]) it has been found that the linearization can be confined to a compact stencil depending only on $\mathbf{q}_i$ and $\mathbf{q}_{i+1}$. This reduces the computational complexity and the memory requirements if the Jacobians are saved. With this two-point stencil for each flux $\mathbf{f}_{i+1/2}$ and $\mathbf{g}_{i+1/2}$, the linearization of the residual with respect to $\mathbf{q}_i$ has a contribution from the flux at each cell face surrounding $\mathbf{q}_i$, and the flux Jacobians can be defined as

$$\mathbf{f}'^{\pm}_i = \frac{\partial\mathbf{f}_{i\pm1/2}}{\partial\mathbf{q}_i}, \quad \mathbf{g}'^{\pm}_j = \frac{\partial\mathbf{g}_{j\pm1/2}}{\partial\mathbf{q}_j}. \tag{5.6}$$

These flux linearizations are evaluated numerically as in the example,

$$k\text{th column of } \mathbf{f}_i'^{\pm} = [\mathbf{f}_{i\pm1/2}(\mathbf{q}_i + h\mathbf{e}_k) - \mathbf{f}_{i\pm1/2}(\mathbf{q}_i)]/h, \quad (5.7)$$

where $\mathbf{e}_k$ is the kth unit vector and $h \approx \sqrt{\text{machine } \varepsilon}$.

It has also been noted by Whitfield and Taylor [11] that a linearization with respect to $\mathbf{q}^{\mathrm{R}}$ and $\mathbf{q}^{\mathrm{L}}$ also works well and is computationally more efficient. In this case, the linearizations are defined by

$$\mathbf{f}_i'^{+} = \frac{\partial \mathbf{f}_{i+1/2}}{\partial \mathbf{q}^{\mathrm{L}}_{i+1/2}}, \quad \mathbf{f}_i'^{-} = \frac{\partial \mathbf{f}_{i-1/2}}{\partial \mathbf{q}^{\mathrm{R}}_{i-1/2}} \quad (5.8)$$

with analogous definitions for $\mathbf{g}'$. The flux linearizations are evaluated as in the example:

$$k\text{th column of } \mathbf{f}_i'^{+}$$
$$= [\mathbf{f}_{i+1/2}(\mathbf{q}^{\mathrm{R}}_{i+1/2}, \mathbf{q}^{\mathrm{L}}_{i+1/2} + h\mathbf{e}_k) - \mathbf{f}_{i+1/2}(\mathbf{q}^{\mathrm{R}}_{i+1/2}, \mathbf{q}^{\mathrm{L}}_{i+1/2})]/h. \quad (5.9)$$

6. ONE-PARAMETER LU/AF ALGORITHM

Having defined the flux approximations and flux Jacobians, the compact linearized flux Jacobian operator can be expressed as

$$\begin{aligned}\mathscr{L}_{i,j}(\cdot) = &-\mathbf{f}_{i-1}'^{+}(\cdot)_{i-1} + (\mathbf{f}_i'^{+} - \mathbf{f}_i'^{-})(\cdot)_i + \mathbf{f}_{i+1}'^{-}(\cdot)_{i+1} \\ &-\mathbf{g}_{j-1}'^{+}(\cdot)_{j-1} + (\mathbf{g}_j'^{+} - \mathbf{g}_j'^{-})(\cdot)_j + \mathbf{g}_{j+1}'^{-}(\cdot)_{j+1}.\end{aligned} \quad (6.1)$$

The definitions of D, $\mathscr{L}_1$, and $\mathscr{L}_2$ appropriate for a one-parameter LU/AF scheme of the type introduced in Section 1 can now be given as

$$D(\cdot) = [(I/\Delta\tau) + \alpha(\mathbf{f}_i'^{+} - \mathbf{f}_i'^{-}) + \alpha(\mathbf{g}_j'^{+} - \mathbf{g}_j'^{-})](\cdot)_{i,j} \quad (6.2a)$$

$$\begin{aligned}\mathscr{L}_1(\cdot) = &(1-\alpha)[\mathbf{f}_i'^{+} + \mathbf{g}_j'^{+}](\cdot)_{i,j} \\ &- \mathbf{f}_{i-1}'^{+}(\cdot)_{i-1} - \mathbf{g}_{j-1}'^{+}(\cdot)_{j-1}\end{aligned} \quad (6.2b)$$

$$\begin{aligned}\mathscr{L}_2(\cdot) = &(1-\alpha)[-\mathbf{f}_i'^{-} - \mathbf{g}_j'^{-}](\cdot)_{i,j} \\ &+ \mathbf{f}_{i+1}'^{-}(\cdot)_{i+1} + \mathbf{g}_{j+1}'^{-}(\cdot)_{j+1}.\end{aligned} \quad (6.2c)$$

It is easily verified that these definitions satisfy (4.7). Here, α is a parameter ($0 \le \alpha \le 1$) which can be adjusted to accelerate convergence. In effect, the parameter α allocates the flux Jacobians associated with the *diagonal* point (i, j) between the elements of the approximate factorization D, $\mathscr{L}_1(\cdot)$, and $\mathscr{L}_2(\cdot)$.

Applying these definitions to the sub-iterative formulation (4.15), the one-parameter LU/AF scheme becomes

$$\begin{aligned}&[I/\Delta\tau + \mathbf{f}_i'^{+} - \alpha\mathbf{f}_i'^{-} + \mathbf{g}_j'^{+} - \alpha\mathbf{g}_j'^{-}]\psi^*_{i,j} - \mathbf{f}_{i-1}'^{+}\psi^*_{i-1} - g'^{+}_{j-1}\psi^*_{j-1} \\ &- (1-\alpha)\mathbf{f}_i'^{-}\psi^m_i + \mathbf{f}_{i+1}'^{-}\psi^m_{i+1} \\ &- (1-\alpha)\mathbf{g}_j'^{-}\psi^m_j + \mathbf{g}_{j+1}'^{-}\psi^m_{j+1} = -\mathbf{R}(\mathbf{q}^n)\end{aligned} \quad (6.3a)$$

$$\begin{aligned}&[I/\Delta\tau + \alpha\mathbf{f}_i'^{+} - \mathbf{f}_i'^{-} + \alpha\mathbf{g}_j'^{+} - \mathbf{g}_j'^{-}]\psi^{m+1}_{i,j} + \mathbf{f}_{i+1}'^{-}\psi^{m+1}_{i+1} + \mathbf{g}_{j+1}'^{-}\psi^{m+1}_{j+1} \\ &+ (1-\alpha)\mathbf{f}_i'^{+}\psi^*_i - \mathbf{f}_{i-1}'^{+}\psi^*_{i-1} \\ &+ (1-\alpha)\mathbf{g}_j'^{+}\psi^*_j - \mathbf{g}_{j-1}'^{+}\psi^*_{j-1} = -\mathbf{R}(\mathbf{q}^n).\end{aligned} \quad (6.3b)$$

For $\alpha = 1$, it can be verified that this scheme is equivalent to symmetric Gauss–Seidel relaxation applied to the iterative time-linearized implicit formulation (4.12) or (4.5). It should be noted that Whitfield [24] has described this scheme with $\alpha = 0$ as the *two-pass* method and with $a = 1$ as the *modified two-pass* method.

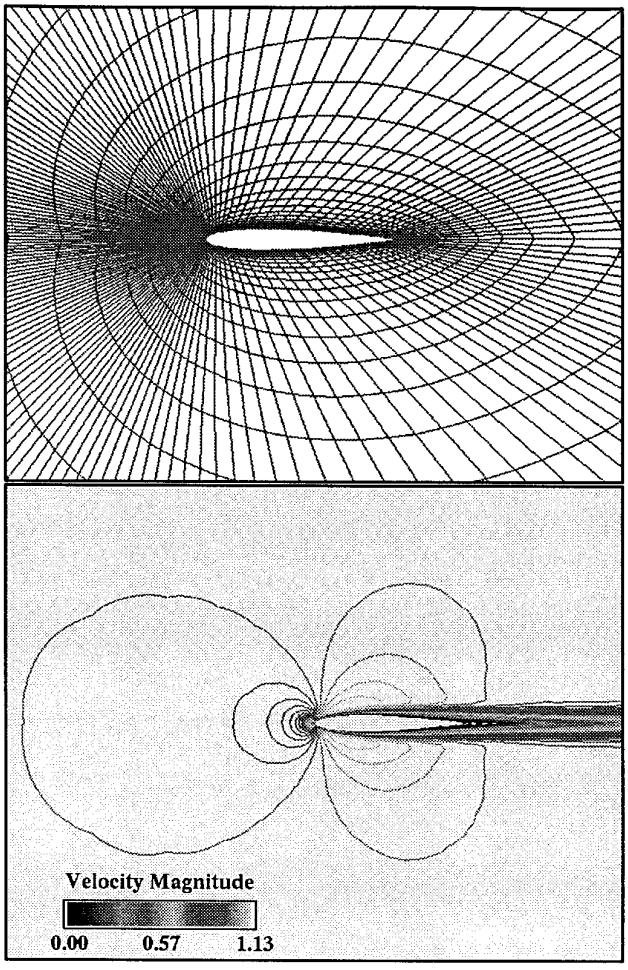

FIG. 3. Grid and computed solution near the airfoil.

7. COMPUTED RESULTS

7.1. *Viscous Flow*

The convergence behavior of the LU/AF scheme was studied for two-dimensional viscous flow past a NACA

TABLE I

Optimal Parameters for Test Problem

	Case 1	Case 2	Case 3	Case 4	Case 5
	Re = 2500 (35 × 161)	Re = 2500 (70 × 161)	Re = 250 (35 × 161)	Re = 250 (70 × 161)	Inviscid (35 × 161)
1 *Sub-Iteration*					
Optimal					
CFL	14 to 19	50 to 80	20 to 100	20 to 100	40
a_{opt}	0.05	0.08	0.05 to 0.2	0.05 to 0.2	0.3
3 *Sub-Iterations*					
Optimal					
CFL	40 to 50	50 to 80	20 to 100	20 to 100	80
a_{opt}	0.1 to 0.2	0.1 to 0.4	0.05 to 0.3	0.05 to 0.2	0.3

TABLE II

Asymptotic Convergence Rate: Iterations to Reduce Residual by a Factor of 10

	Case 1	Case 2	Case 3	Case 4	Case 5
	Re = 2500 (35 × 161)	Re = 2500 (70 × 161)	Re = 250 (35 × 161)	Re = 250 (70 × 161)	Inviscid (35 × 161)
1 *Sub-Iteration*					
$a = 1$	533	174	213	256	91
a_{opt}	125	81	70	60	49
3 *Sub-Iterations*					
$a = 1$	61	59	148	154	32
a_{opt}	34	29	19	22	22

0012 airfoil at zero incidence (see Fig. 3). A large number of test calculations were made for each of five flow cases in which the grid resolution and Reynolds number were varied (see Table I). The first case has a chordal Reynolds number of 2500 and uses an O-grid with 35 radial points and 161 circumferential points. The outer boundary of the grid is a circle with radius 50 times the airfoil chord length. The grid is very highly stretched to provide resolution of the viscous layer, leading and trailing edge regions. For Case 1, the minimum mesh spacing is a 5.7×10^{-4} chord for the radial direction and an 8.7×10^{-5} chord for the circumferential direction. The ratio of minimum to maximum mesh spacing is about 7.1×10^{-5} for the radial direction and 3.6×10^{-5} for the circumferential direction. The ratio of the maximum to minimum cell areas is 1.2×10^{10}. The artificial compressibility parameter β was taken as 5.0. The iterative time-linearized LU/AF scheme given by (6.3a), (6.3b) was used. This scheme, the same as (4.15a), (4.15b), is equivalent to (4.14a), (4.14b) and, with one sub-iteration, is equivalent to (4.8a)–(4.8b), as noted in Section 4. The calculations were performed using third-order numerical fluxes as in (5.4a)–(5.4b) and numerical flux linearizations were updated numerically every 20 time steps. A spatially varying time step was used and is defined as

$$\Delta t_{i,j} = \mathrm{CFL}[|\lambda_i|_{\max} + |\lambda_j|_{\max}]^{-1},$$

where λ_i and λ_j are the eigenvalues of $\overline{\mathbf{A}}$ and $\overline{\mathbf{B}}$, and CFL is a specified constant. Characteristic-based boundary conditions are used as described in [11].

To make a meaningful assessment of convergence behavior, it is necessary to determine the optimal value of time step (CFL) for each choice of parameter α. This was done empirically by trial and error using different values of CFL and α and computing enough time steps to determine the relevant asymptotic convergence behavior. The convergence behavior for $\alpha = 1$ (equivalent to symmetric Gauss–Seidel relaxation) was first determined and then compared with the corresponding behavior for other values of α. A large number of test calculations were made for each of the five cases, and key results are summarized in Table I and Table II.

For Case 1, detailed results for variable CFL and α are shown in Figs. 4–5. For one sub-iteration, the optimal CFL for $\alpha = 1$ was found to be 14, and the optimal parameter α_{opt} was 0.05, with the optimal CFL of 19. For three sub-iterations, the optimal CFL for $\alpha = 1$ was 45, and the optimal parameter α_{opt} was 0.1, with the optimal CFL of 42. The convergence behavior for this case is shown in Fig. 6. For one sub-iteration, the asymptotic rate of convergence to a steady solution using $\alpha_{opt} = 0.05$ is improved by a factor of about 4, as compared with that for $\alpha = 1$. For three sub-iterations, the convergence is improved by a factor of about 2 using $\alpha_{opt} = 0.1$.

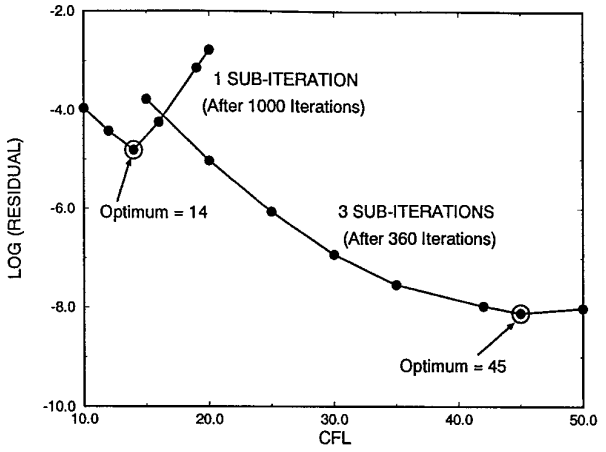

FIG. 4. Case 1: Determination of optimal CFL for $a = 1$ from reduction of initial residual.

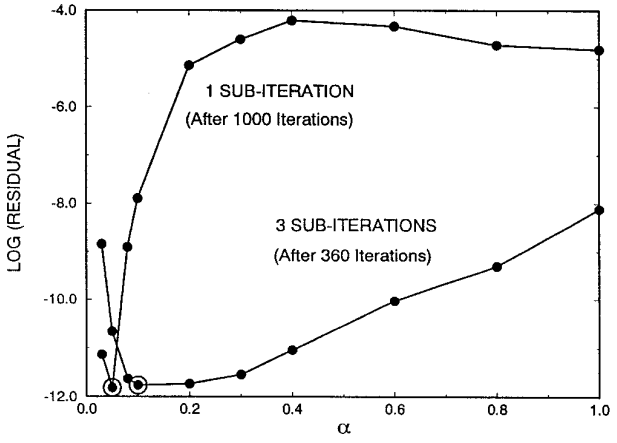

FIG. 5. Case 1: Determination of optimal a from reduction of initial residual, using optimal CFL for each a.

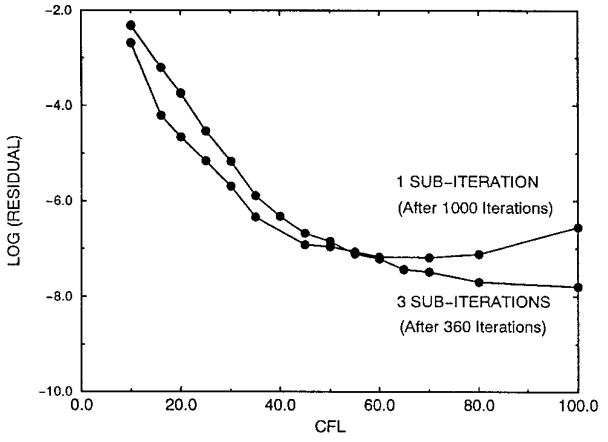

FIG. 7. Case 2: Determination of optimal CFL for $a = 1$ from reduction of initial residual.

For Case 2, the local radial mesh spacing is halved, improving the viscous resolution, with minimum mesh spacing of a 2.85×10^{-4} chord. The results for variable CFL and α are shown in Figs. 7–8, and by comparison with Figs. 4–5, the algorithm generally has an improved convergence behavior for one sub-iteration. A lower Reynolds number (250) is used for Cases 3 and 4, giving better viscous resolution. Since the results for Cases 3 and 4 are very similar, only Case 4 results for variable CFL and α are shown (Figs. 9–10). Comparing these results with Figs. 4–5 and Figs. 7–8, the algorithm can be seen to have an improved convergence behavior for both the (35×161) and (70×161) grids at the lower Reynolds number.

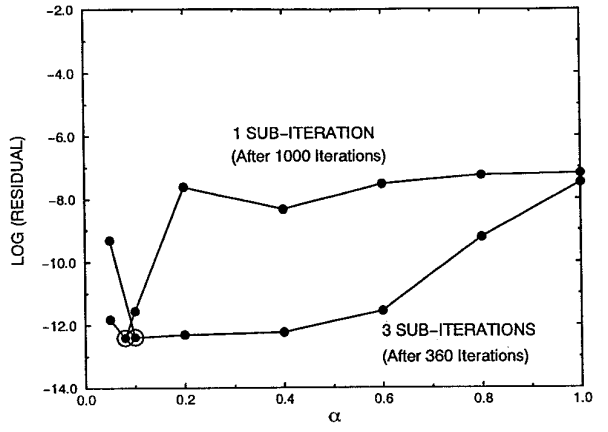

FIG. 8. Case 2: Determination of optimal a from reduction of initial residual, using optimal CFL for each a.

7.2. *Inviscid Flow*

Computed results were also obtained for inviscid flow with the (35×161) grid (Case 5). The only changes in

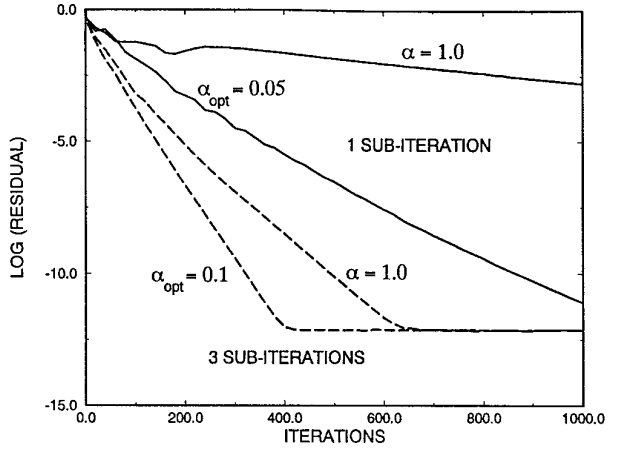

FIG. 6. Case 1: Viscous flow convergence behavior at optimal CFL.

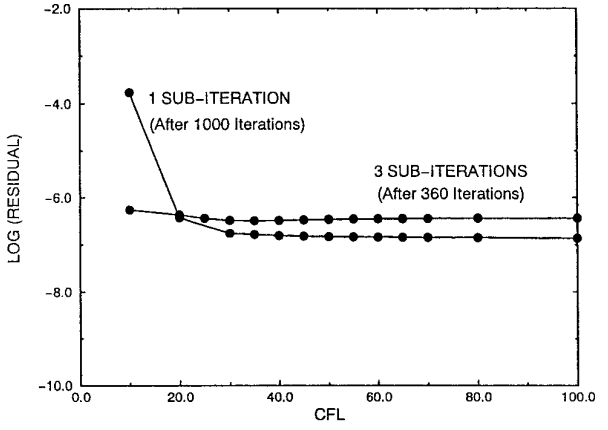

FIG. 9. Case 4: Determination of optimal CFL for $a = 1$ from reduction of initial residual.

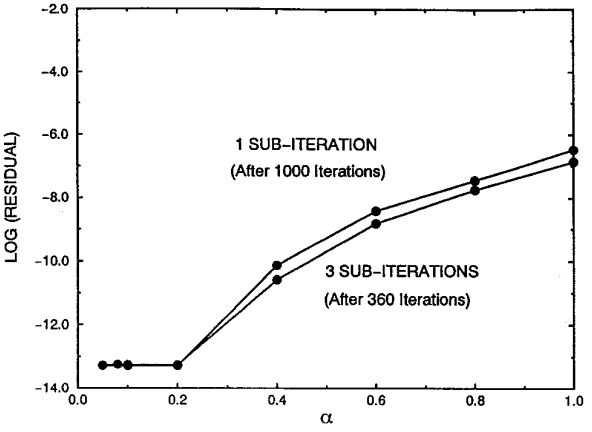

FIG. 10. Case 4: Determination of optimal *a* from reduction of initial residual, using optimal CFL for each *a*.

computing the inviscid solution are the omission of all the viscous terms in the governing equations and the use of inviscid boundary conditions at the airfoil surface. The convergence behavior for these calculations is shown in Fig. 11. As in the viscous case, the convergence rate is improved using optimal parameters. The results summarized in Table II show that the convergence rate is improved in all cases using $\alpha = \alpha_{opt}$. The inviscid cases for $\alpha = 1$ all converged 2–5 times faster than the viscous cases, but there was much less difference for $\alpha = \alpha_{opt}$.

8. CONCLUDING REMARKS

For the specific test problem considered here, it has been found that the iteration parameter α in the present LU/AF scheme can be adjusted to improve the iterative convergence rate. Although it is not feasible to determine optimal parameter values in large-scale practical calculations, it does not appear difficult to guess a useful value. A value for α near 0.05 to 0.2 has usually given good performance, although the scheme does not work well if α is too small. The optimal CFL number may vary with the number of sub-iterations but it does not seem sensitive to α. In terms of total iterations (time steps plus sub-iterations), it is better to avoid sub-iteration and use α_{opt}. In terms of computer resources (CPU time and memory), there is a trade-off between reducing the runtime for sub-iterations by storing and reusing quantities such as flux linearizations and residuals and the increased memory required to do this.

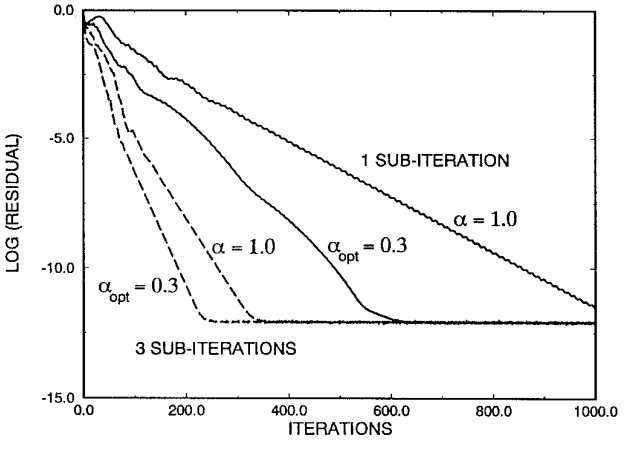

FIG. 11. Case 5: Inviscid flow: Convergence behavior at optimal CFL.

ACKNOWLEDGMENTS

This work was sponsored by the National Science Foundation, Division of Advanced Scientific Computing. The authors wish to thank Lafe K. Taylor for providing a version of the inviscid incompressible flow solver described in [11], modified to include viscous terms as described in [10].

REFERENCES

1. A. J. Chorin, *J. Comput. Phys.* **2,** 12 (1967).
2. S. E. Rogers and D. Kwak, *AIAA J.* **28,** 253 (1990).
3. M. M. Athavale and C. L. Merkle, AIAA Paper No. 88-3650, 1988 (unpublished).
4. W. R. Briley, R. C. Buggelin, and H. McDonald, "Solution of the Incompressible Navier–Stokes Equations Using Artificial Compressibility," in *Proceedings, 11th International Conference on Numerical Methods in Fluid Mechanics, Williamsburg, Virginia, 1988,* edited by D. L. Dwoyer, M. Y. Hussaini, and R. G. Voigt (Springer-Verlag, New York, 1989).
5. L. K. Taylor and D. L. Whitfield, AIAA Paper No. 91-1650, 1991 (unpublished).
6. S. E. Rogers, D. Kwak, and C. Kiris, *AIAA J.* **29,** 603 (1991).
7. A. Jameson and E. Turkel, *Math Comput.* **37,** 385 (1981).
8. A. Jameson, "Successes and Challenges in Computational Aerodynamics," in *Proceedings, 8th Computational Fluid Dynamics Conference, Honolulu, HI* (Am. Inst. Aeronautics and Astronautics, Washington, DC, 1987), p. 1.
9. S. Yoon and D. Kwak, *AIAA J.* **29,** 874 (1991).
10. L. K. Taylor, J. A. Busby, M. Y. Jiang, A. Arabshahi, K. Sreenivas, and D. L. Whitfield, "Time-Accurate Incompressible Navier–Stokes Simulation of the Flapping Foil Experiment," in *Proceedings, Sixth International Conference on Numerical Ship Hydrodynamics, Iowa City, Iowa, 1993,* edited by V. C. Patel and F. Stern (National Acad. Press, Washington, DC, 1994).
11. D. L. Whitfield and L. K. Taylor, Mississippi State Univ. Report No. MSSU-EIRS-ERC-93-14, 1994 (unpublished).
12. D. Pan and H. Lomax, *AIAA J.* **26,** 163 (1988).
13. S. Yoon and A. Jameson, *AIAA J.* **26,** 1025 (1988).
14. T. I-P. Shih, E. Steinthorsson, and W. J. Chyu, *AIAA J.* **31,** 788 (1993).
15. P. L. Roe, *J. Comput. Phys.* **43,** 357 (1981).
16. B. van Leer, *J. Comput. Phys.* **32,** 101 (1979).
17. W. K. Anderson, J. T. Thomas, and B. van Leer, *AIAA J.* **24,** 1453 (1986).
18. D. L. Whitfield and L. K. Taylor, AIAA Paper No. 91-1539, 1991 (un-

published).

19. A. Jennings, *Matrix Computation for Engineers and Scientists* (Wiley, New York, 1977), p. 289.
20. F. M. White, *Viscous Fluid Flow,* 2nd ed. (McGraw–Hill, New York, 1991).
21. W. R. Briley and H. McDonald, *J. Comput. Phys.* **24,** 372 (1977).
22. J. M. Ortega and W. C. Rheinboldt, *Iterative Solution of Nonlinear Equations in Several Variables* (Academic Press, New York, 1970).
23. D. Pan and S. Chakravarthy, AIAA Paper No. 89-0122, 1989 (unpublished).
24. D. L. Whitfield, Mississippi State Univ. Report No. MSSU-EIRS-ASE-90-3, 1990 (unpublished).